

# Field Verification of Acoustic Doppler Surface Gravity Wave Measurements

T. H. C. HERBERS, R. L. LOWE, AND R. T. GUZA

*Center for Coastal Studies, Scripps Institution of Oceanography, La Jolla, California*

A compact acoustic Doppler current meter, designed for nearshore surface gravity wave measurements, was field tested by comparison to a collocated array of pressure transducers. Both measurement systems were bottom mounted in a water depth of 7 m. Each of four acoustic beams, inclined 45° from vertical, measures the along-beam velocity at a single range (1 m) about 1.5 m above the seafloor. These four velocity beams are used to estimate low-order moments of the frequency-directional wave spectrum and are compared to pressure measurements on four occasions. Predictions of the (nondirectional) bottom pressure spectrum at sea and swell frequencies (0.04–0.30 Hz), based on the velocity measurements and linear theory, are in excellent agreement with directly measured pressure. The general level of agreement (gain errors less than 5%) is somewhat better than results reported from similar (but spanning a much wider range of conditions) intercomparison studies using conventional in situ current meters. Observed cross spectra between collocated pressure and horizontal velocity components, frequently used to separate turbulence and wave orbital velocities (assuming that the coherence of wave velocity and pressure is equal to 1), are compared to predictions based on the pressure array data and linear wave theory. The observed and predicted pressure-velocity cross spectra are in excellent agreement and show that large coherence reductions can occur in natural wind waves owing to wave directional spreading effects, despite relatively low turbulence energy levels. Wave radiation stresses, estimated from the velocity measurements, also agree well with estimates extracted from the pressure array data. Overall, the intercomparisons show that the present acoustic Doppler system has directional resolution comparable to a pitch-and-roll buoy, and they suggest that higher-order directional information as well as weak nonlinear properties of natural wind waves may be examined with a slightly modified compact system.

## 1. INTRODUCTION

The frequency-directional spectrum of sea and swell can be accurately estimated with spatially extensive arrays of pressure transducers or current meters (for example, Pawka [1983], Allender *et al.* [1989], Herbers and Guza [1990] and others). However, these arrays are expensive to deploy and maintain, and generally, they require spatially uniform wave statistics over their entire aperture (several hundred meters for high resolution of long swell, a condition not always met in nearshore waters). The difficulty of deploying large in situ arrays is reflected in the relatively few times they have been implemented.

Point systems, such as the pitch-and-roll buoy [Longuet-Higgins *et al.*, 1963], pressure sensor–current meter combination (hereafter "PUV" system [Nagata, 1964; Bowden and White, 1966]) and "slope array" [Higgins *et al.*, 1981], are more suitable for routine applications and have been widely used to sample wave directional statistics. These measurement systems have formally equivalent (and relatively poor) directional resolution but can provide bulk directional wave data useful in studies of a variety of nearshore processes. For example, these systems yield accurate estimates of radiation stresses, the depth-averaged excess momentum fluxes due to surface gravity waves [Longuet-Higgins and Stewart, 1962], believed to be the principal driving forces for wave setup, longshore currents, and sediment transport.

Slope arrays, routinely deployed at various coastal sites [Seymour *et al.*, 1985], are very reliable but can provide accurate radiation stress estimates only for a limited frequency range. For wavelengths much larger than the array dimension the estimates are sensitive to instrument noise while for short wavelength waves the curvature of the sea surface between the pressure sensors introduces a bias [Herbers and Guza, 1989].

PUV gauges do not have this frequency range limitation, but electromagnetic current meters (hereafter "EM") frequently used in these systems are much less reliable, are difficult to calibrate, are susceptible to biological fouling [e.g. Grosskopf *et al.*, 1983; Guza *et al.*, 1988], and may distort the measured flow field. Acoustic travel time current meters (hereafter "ATT") can work well in PUV systems but have been reported to have problems with air bubbles [Derks and Stive, 1984] and biofouling [Allender *et al.*, 1989]. In addition to the difficulty of maintaining these instruments in the field, both EM and ATT current meters are intrusive, somewhat distorting the measured flow field. The accuracy of the calibration for instrument gain (e.g., instrument voltage output per centimeters per second of flow) is estimated at roughly  $\pm 5\%$  for both instruments [Battjes and Van Heteren, 1984; Derks and Stive, 1984; Guza *et al.*, 1988]. However, field comparisons of EM and ATT current meter gains to pressure or surface elevation measurements (based on linear theory) show errors that are typically  $\pm 10\%$  at the spectral peak frequency and can be significantly larger at twice the peak frequency [e.g., Guza and Thornton, 1980; Battjes and Van Heteren, 1984]. How much of this uncertainty is due to wave nonlinearity, turbulence, or the limitations of these current meters is unknown. Although acceptable for estimating gross wave statistics, the accuracy and linearity of these sensors is not suitable for all applications.

There have been several extensive studies which intercompared various compact directional wave measurement systems, including pitch-and-roll buoys, slope arrays, and PUV gauges with both EM and ATT current meters. In general these systems performed well [Grosskopf *et al.*, 1983; Derks and Stive, 1984; Allender *et al.*, 1989], with agreement between estimates of the peak direction and the directional spread (at the peak frequency). Comparisons of an ATT current meter and a three-element pressure gauge array reported by Van Heteren *et al.* [1988] show fair agreement between estimates of peak directions but large discrepancies between estimates of the directional spread, possibly due to relatively high noise levels in the measurements. It is noteworthy that

Copyright 1991 by the American Geophysical Union.

Paper number 91JC01326.  
0148-0227/91/91JC-01326\$05.00

estimates of peak direction and spread (for a given frequency) depend only on the lowest-order Fourier coefficients  $a_1$  and  $b_1$  of the directional distribution  $S(\theta)$

$$a_n = \int_0^{2\pi} d\theta \cos(n\theta) S(\theta) \quad (1a)$$

$$b_n = \int_0^{2\pi} d\theta \sin(n\theta) S(\theta) \quad (1b)$$

The intercomparison studies did not include the higher-order coefficients (i.e.,  $a_2$  and  $b_2$ ) produced by pitch-and-roll type systems. Nonetheless, a variety of compact systems appear to function reasonably well at the pitch-and-roll level of resolution.

Point measurement systems with theoretically higher resolution ( $a_3$ ,  $b_3$ ,  $a_4$ , and  $b_4$  are obtained in principal) have been deployed. These systems attempt to measure either second derivatives of sea surface elevation (i.e., surface curvature [Cartwright and Smith, 1964; Mitsuyasu et al., 1975; Bodge and Dean, 1984]) or first derivatives of the two horizontal components of wave velocity [Simpson, 1969]. Unfortunately, none of the measurements have apparently been accurate enough to yield meaningful results. The problem with measuring sea surface curvature is basically one of signal to noise; sea surface elevation is readily measured with good accuracy, sea surface slope is more difficult because it is obtained by taking the small difference of nearby surface elevations, and curvature is even harder still since it is based on the small difference of nearby relatively inaccurate surface slope measurements [Bodge and Dean, 1984]. Measuring first differences of wave velocity has been hampered by the relative difficulty of accurately measuring wave-induced velocity.

In this study a field verification is presented of an alternative compact measurement system, an acoustic Doppler current meter (hereafter "AD") developed to measure horizontal orbital wave velocities. Acoustic Doppler velocity measurements have several advantages over conventional nearshore wave measurement systems. Unlike EM and ATT current meters, the AD sample volume is not in close proximity to the instrument itself. Hence, distortion of the measured flow field by the instrument is avoided, and in principal very accurate measurements, potentially useful for studies of weak nonlinear effects on surface waves, can be obtained. The response of the AD current meter is a linear function of the speed of sound which depends on the temperature and (very weakly) on the salinity of seawater. A calibration is not required for the AD current meter. A crude estimate of the water temperature (within  $\pm 5^\circ\text{C}$ ) is sufficient to determine the instrument gain with an accuracy of 1%. The AD current meter may also be less sensitive than EM or ATT current meters to biofouling.

Another advantage of AD velocity measurements is the potential to observe wave velocities at multiple positions, in either the horizontal (useful for estimating directional wave spectra) or vertical planes, with a single range-gated instrument that is easier to deploy and maintain than conventional arrays of pressure transducers or current meters. Krogstad et al. [1988] present a comparison of directional wave data from a range-gated AD current meter and a PUV system using an EM current meter. They found reasonable agreement of peak direction and directional spread, despite high noise levels in the AD velocity measurements. Range-gated AD systems (see also Pinkel and Smith [1987]) potentially have a resolution comparable to extensive spatial arrays, but these complex systems are still under development.

The relatively simple AD current meter developed in the present study measures the along-beam velocity at a single range

of 1 m along each of four acoustic beams, inclined  $45^\circ$  from vertical. The instrument was mounted on the seabed in 7 m depth, embedded in an array of pressure transducers that provides "ground truth" directional wave data. The basic accuracy of the AD measurements is established with comparisons of observed and predicted (using the AD data and linear theory) pressure spectra. Data from the four beams can be combined to yield a single point measurement of two orthogonal horizontal velocity components, comparable to a conventional biaxial EM or ATT current meter. The performance of a PUV system, formed by these estimates of horizontal currents and a collocated pressure sensor, is verified by comparing estimates of the low-order Fourier coefficients  $a_1$ ,  $b_1$ ,  $a_2$ , and  $b_2$  (equation (1)) to estimates obtained from the pressure array data. The results generally show excellent agreement and suggest that acoustic Doppler techniques are indeed a promising alternative for nearshore directional wave measurements. Minor modifications to the instrument may further improve its performance and allow estimation of higher-order directional wave information. The AD instrument is described in section 2, followed by a description of the field experiment and the analysis methodology in section 3. Comparisons of acoustic Doppler and pressure measurements are presented in section 4, followed by a discussion in section 5. The results are summarized in section 6.

## 2. INSTRUMENT DESCRIPTION

An acoustic Doppler current meter was developed for measuring orbital wave velocities. The instrument contains four pairs (i.e., transmitter and receiver) of 1-MHz acoustic transducers in two 30-cm-long PVC (polyvinylchloride) bars, orthogonally mounted on top of an aluminum cylinder housing the electronics (Figure 1a). Each transducer pair ensonifies a measurement volume centered about 1 m from the instrument (Figure 1b). The beams look outward from the instrument case axis at a  $45^\circ$  angle, resulting in velocity measurements at the four corners of a 1-m square in the horizontal plane (Figure 1a). A small fraction of the transmitted sound energy is backscattered from small suspended organic and inorganic particles (found in abundance in coastal waters) advected with the wave orbital motion. The fluid velocity component directed in the plane of the acoustic beams, along the bisect of the transmitted and reflected beams (Figure 1), causes a Doppler shift in the frequency of received sound. The transmitters send a pulse of sound energy with a 1-ms duration at 5-ms intervals. To eliminate contamination of the backscattered sound by leakage of transmitted sound into the receiver, the receiver listens only when the transmitter is off. The details of the data processing, applied to the received sound, are described by Lowe and Guza [1990]. Both coherent and incoherent processing schemes were applied to the present data [Lhermitte, 1985; Smith, 1989]. The coherent processing used in the following intercomparisons resulted in a relatively low spectral noise level of about  $0.1 \text{ (cm/s)}^2/\text{Hz}$ , compared to noise levels of about  $10 \text{ (cm/s)}^2/\text{Hz}$  for incoherent processing of the same data and  $1 \text{ (cm/s)}^2/\text{Hz}$  for a Marsh-McBirney electromagnetic current meter in an electromagnetically quiet environment [Guza et al., 1988]. Using incoherent processing with a range-gated AD current meter, Krogstad et al. [1988] observed a noise level of about  $50 \text{ (cm/s)}^2/\text{Hz}$ .

In the present deployment, the electronics package of the AD current meter was mounted on the seafloor in 7-m depth, and the data were cabled to a personal computer on a nearby pier. The sample volumes of the four acoustic beams were located 1.5 m above the bed and approximately aligned with the local depth con-

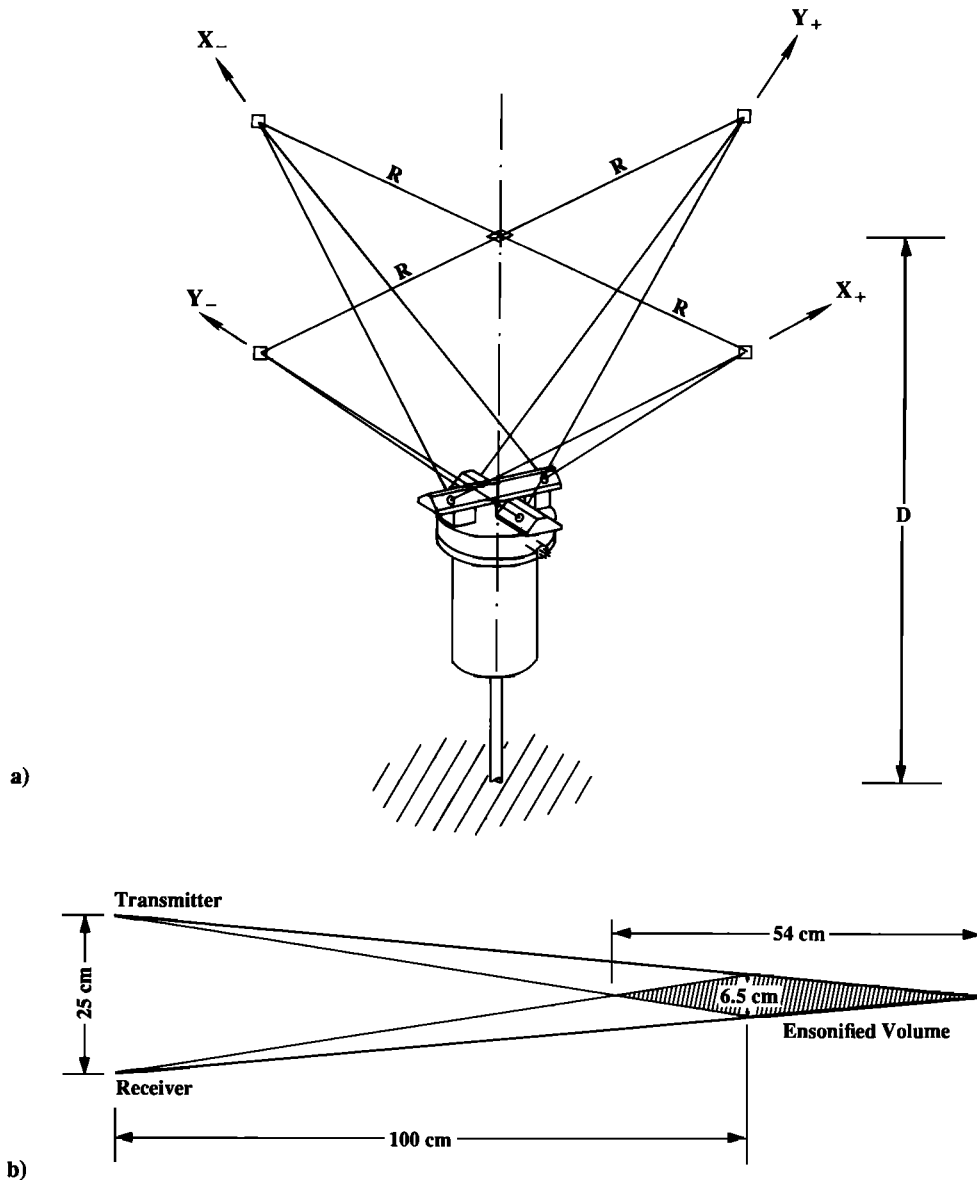


Fig. 1. Schematic of the acoustic Doppler velocimeter. (a) The geometry of the instrument with four beam pairs ( $X_+$ ,  $X_-$ ,  $Y_+$ , and  $Y_-$ ) and the locations where velocities are measured are shown. The horizontal distance between the instrument axis and each sample volume ( $R = 0.7$  m) and the elevation of the measurements above the bed ( $D = 1.5$  m) are also illustrated, as well as (b) the plan view of the ensonified volume formed by the intersection of a transmitter/receiver beam pair.

tours (Figure 1). Even though side lobes of the acoustic beams are attenuated by about  $10^4$  at the sea surface, surface reflections are strong enough to seriously contaminate the received sound. The simultaneous arrival at the receivers, of sound scattered from the sample volumes and side lobe reflections of past pulses from the sea surface, sometimes gave degraded velocity measurements. Acoustic shielding of the instrument reduced this surface interference, but degraded return signals were sometimes observed at low tide. Low tide data are excluded from the following discussion. Work in progress modifies the timing of the transmitted pulses so that the arrivals of sound scattered from the sample volumes and surface (side lobe) reflections are well separated in time. Preliminary results suggest that the surface interference can be effectively eliminated for a limited range of tidal fluctuations (roughly  $\pm 1$  m) about the mean (7 m) depth.

The  $X_+$  and  $X_-$  beams of the AD current meter contain the cross-shore velocity component ( $u$ ), and the  $Y_+$  and  $Y_-$  beams

contain the longshore component ( $v$ ); the vertical component ( $w$ ) contributes to the signal of all four beams (Figure 1). Since the four AD velocity measurements are spatially separated (Figure 1), they generally cannot be simply combined to yield  $u$ ,  $v$ , and  $w$  (i.e., equivalent to a triaxial current meter). However, for surface wavelengths much larger than the separation of the sample volumes, variations in the wave orbital velocity field between the four measurements are theoretically relatively small so that the beam differences  $X_+ - X_-$  and  $Y_+ - Y_-$  approximately yield  $u\sqrt{2}$  and  $v\sqrt{2}$ , respectively (Figure 1a). Similarly, for relatively long waves the beam sums  $X_+ + X_-$  and  $Y_+ + Y_-$  both approximately yield  $w\sqrt{2}$  (Figure 1a), but if the height of the measurements above the sea bed is very small compared to the wavelength, then  $w < [u^2 + v^2]^{1/2}$  and variations in  $u$  and  $v$  between the sample volumes may be comparable to  $w$ .

The present AD system (including a pressure sensor at the instrument center) was designed to provide low-order Fourier

coefficients ( $a_n, b_n$ ; equation (1)) of the directional wave spectrum. To estimate these moments from the AD measurements and examine the bias in the estimates resulting from the finite separation of the four sample volumes, it is useful to expand the  $X_+, X_-, Y_+$  and  $Y_-$  velocity measurements about the instrument center. For small  $kR$ , where  $k$  is the wave number and  $R$  is the horizontal distance between the instrument axis ( $x = y = 0$ ) and each sample volume (Figure 1a), the velocities measured by the cross-shore beams are

$$\sqrt{2} X_+ = (u + w) \Big|_{x=R, y=0, z=D} = u + w + R(u_x + w_x) + \frac{R^2}{2}(u_{xx} + w_{xx}) + \frac{R^3}{6}(u_{xxx} + w_{xxx}) + \dots \Big|_{x=0, y=0, z=D} \quad (2a)$$

$$\sqrt{2} X_- = (-u + w) \Big|_{x=-R, y=0, z=D} = -u + w - R(-u_x + w_x) + \frac{R^2}{2}(-u_{xx} + w_{xx}) - \frac{R^3}{6}(-u_{xxx} + w_{xxx}) + \dots \Big|_{x=0, y=0, z=D} \quad (2b)$$

The longshore beams  $Y_+$  and  $Y_-$  are given by similar equations. The subscripts  $x$  and  $y$  denote differentiation with respect to  $x$  and  $y$ , respectively, and  $D$  is the elevation of the velocity measurements above the bed (Figure 1a). The difference between the  $X_+$  and the  $X_-$  ( $Y_+$  and  $Y_-$ ) velocity measurements is approximately proportional to  $u$  ( $v$ ):

$$X_{diff} \equiv \frac{X_+ - X_-}{\sqrt{2}} = u + R w_x + \frac{R^2}{2} u_{xx} + \frac{R^3}{6} w_{xxx} + \dots \quad (3a)$$

$$Y_{diff} \equiv \frac{Y_+ - Y_-}{\sqrt{2}} = v + R w_y + \frac{R^2}{2} v_{yy} + \frac{R^3}{6} w_{yyy} + \dots \quad (3b)$$

To examine the bias contributed by velocity derivative terms, it is useful to express (3) in the frequency domain. For linear surface gravity waves, orbital velocities and their derivatives may be written as directional moments of the bottom pressure Fourier-Stieltjes transform  $dP(\mathbf{k})$ :

$$X_{diff}(t) = \int_{-\infty}^{\infty} \int_{-\infty}^{\infty} dP(\mathbf{k}) \exp[-2\pi i f t] \cosh(kD) \frac{gk}{2\pi f} \cdot \left[ [1 + kR \tanh(kD)] \cos(\theta) - \frac{(kR)^2}{2} \left[ 1 + \frac{kR}{3} \tanh(kD) \right] \cos^3(\theta) + O(kR)^4 \right] + c.c. \quad (4a)$$

$$Y_{diff}(t) = \int_{-\infty}^{\infty} \int_{-\infty}^{\infty} dP(\mathbf{k}) \exp[-2\pi i f t] \cosh(kD) \frac{gk}{2\pi f} \cdot \left[ [1 + kR \tanh(kD)] \sin(\theta) - \frac{(kR)^2}{2} \left[ 1 + \frac{kR}{3} \tanh(kD) \right] \sin^3(\theta) + O(kR)^4 \right] + c.c. \quad (4b)$$

where  $\mathbf{k}$  is the vector wave number ( $k \cos\theta, k \sin\theta$ ),  $f$  is the frequency given by the surface gravity wave dispersion relation, and c. c. denotes the complex conjugate of the right-hand side expression. The  $O(1)$ ,  $O(kR)$ ,  $O(kR)^2$ , and  $O(kR)^3$  terms in (4a) correspond to the  $u$ ,  $w_x$ ,  $u_{xx}$ , and  $w_{xxx}$  terms in (3a), and the

correspondence of terms is similar in (3b) and (4b). Note that  $w_x$  and  $w_y$  have the same directional dependence as  $u$  ( $\cos\theta$ ) and  $v$  ( $\sin\theta$ ). For  $kR \ll 1$ , the higher order  $\cos^3\theta$  ( $u_{xx}$ ) and  $\sin^3\theta$  ( $v_{yy}$ ) terms may be neglected, and the  $X_{diff}$  and  $Y_{diff}$  measurements are equivalent to a biaxial ( $u, v$ ) current meter with a slightly higher gain ( $1 + kR \tanh[kD]$ ; equation (4)) due to the  $w_x$  and  $w_y$  contributions. The AD beam differences combined with a pressure (or surface elevation) measurement at  $x = 0, y = 0$  thus form a PUV system. The lowest-order Fourier coefficients  $a_1, b_1, a_2$ , and  $b_2$  of the directional distribution  $S(\theta)$  (equation (1)) can be expressed in terms of the cospectra of  $X_{diff}, Y_{diff}$  and a colocated pressure sensor. For the present system  $kR < 0.25$  for  $f < 0.3$  Hz so that the  $O(kR)^2$  velocity curvature terms in (4), neglected in this approximation, are indeed very small ( $< 0.03$ ) in the sea and swell frequency range (0.04–0.30 Hz) considered in this study.

Higher-order directional wave data can be obtained from  $x$  and  $y$  derivatives of  $u$  and  $v$ . The gradients  $u_x$  and  $v_y$  are contained in the beam sums (equation (2))

$$X_{sum} \equiv \frac{X_+ + X_-}{\sqrt{2}} = w + R u_x + \frac{R^2}{2} w_{xx} + \frac{R^3}{6} u_{xxx} + \dots \quad (5a)$$

$$Y_{sum} \equiv \frac{Y_+ + Y_-}{\sqrt{2}} = w + R v_y + \frac{R^2}{2} w_{yy} + \frac{R^3}{6} v_{yyy} + \dots \quad (5b)$$

Analogous to (3) and (4), the beam sums are expressed in the frequency domain in terms of directional moments of the bottom pressure field

$$X_{sum}(t) = \int_{-\infty}^{\infty} \int_{-\infty}^{\infty} dP(\mathbf{k}) \exp[-2\pi i f t] \cosh(kD) i \frac{gk}{2\pi f} \cdot \left[ -\tanh(kD) + kR \left[ 1 + \frac{kR}{2} \tanh(kD) \right] \cos^2(\theta) - \frac{(kR)^3}{6} \cos^4(\theta) + O(kR)^4 \right] + c.c. \quad (6a)$$

$$Y_{sum}(t) = \int_{-\infty}^{\infty} \int_{-\infty}^{\infty} dP(\mathbf{k}) \exp[-2\pi i f t] \cosh(kD) i \frac{gk}{2\pi f} \cdot \left[ -\tanh(kD) + kR \left[ 1 + \frac{kR}{2} \tanh(kD) \right] \sin^2(\theta) - \frac{(kR)^3}{6} \sin^4(\theta) + O(kR)^4 \right] + c.c. \quad (6b)$$

where the  $O(1)$ ,  $O(kR)$ ,  $O(kR)^2$ , and  $O(kR)^3$  terms in (6a) correspond to the  $w$ ,  $u_x$ ,  $w_{xx}$ , and  $u_{xxx}$  terms in (5a), and the correspondence is similar for (5b) and (6b). Since the  $w$ ,  $w_{xx}$ , and  $w_{yy}$  contributions to (6) have the same directional dependence as  $p$  (1),  $u_x$  ( $\cos^2\theta$ ), and  $v_y$  ( $\sin^2\theta$ ), respectively, and the higher-order  $\cos^4\theta$  ( $u_{xxx}$ ) and  $\sin^4\theta$  ( $v_{yyy}$ ) terms are very small for  $kR \ll 1$ , estimates of the Fourier coefficients  $a_3, b_3$ , and  $a_4$  of the directional distribution  $S(\theta)$  (equation (1)) can in principle be extracted from the cross spectra of  $X_{diff}, Y_{diff}, X_{sum}, Y_{sum}$ , and a colocated pressure sensor (equations (4) and (6)). Since the velocity gradients  $u_x$  and  $v_x$  are not measured with the present beam geometry,  $b_4$  cannot be extracted.

For the very small separation of the sample volumes in the present AD current meter ( $kR = 0.02$ – $0.25$  in the frequency range

0.04–0.30 Hz), the  $O(kR)^3$  bias terms in (6) are indeed negligibly small. However, the  $O(kR)$   $u_x$  and  $v_y$  measurements based on the beam sums (equation (6)) are expected to be much more sensitive to instrument noise and therefore less accurate than the  $O(1)$   $u$  and  $v$  measurements based on the beam differences (equation (4)). Increasing  $R$  will reduce the sensitivity to noise of velocity gradients extracted from the  $X_{sum}$  and  $Y_{sum}$  measurements, but it will also increase bias errors due to neglected higher-order terms in the small  $kR$  expansion (equations (4) and (6)). Future work will involve the development and testing of a modified AD current meter with a larger separation of the sample volumes, suitable for accurate velocity gradient measurements. Improved estimators, based on (4) and (6), that minimize the finite  $kR$  bias errors (analogous to *Herbers and Guza* [1989] for slope arrays), will be used for calculating directional information.

3. EXPERIMENT AND ANALYSIS METHOD

To verify that the new acoustic Doppler instrument can accurately measure orbital velocities of surface gravity waves, a field experiment was conducted near the end of the Scripps Institution of Oceanography pier during summer 1989. The AD current meter was deployed in a water depth of approximately 7 m  $\pm$  0.5 m tidal fluctuations, embedded in a nine-element ground truth array (32 m x 32 m aperture) of capacitance sensing pressure transducers (Figure 2). The pressure sensors were mounted 0.5 m above the sea bed and sampled at 4 Hz. Depth variations across the array are less than 1 m. Comparisons of frequency spectra computed for the individual pressure sensors, as well as the cross spectra of redundant array lags, generally show excellent agreement, confirming that the wave statistics are spatially uniform across the array. A single pressure transducer ( $P_{10}$ , Figure 2),

was positioned as close as possible to the AD current meter to form a PUV system. Simultaneous PUV (AD current meter and  $P_{10}$ ) and pressure array data were collected for approximately 1 hour on each of four days (August 30, and September 7, 8, and 11). On all four occasions waves were believed to be small enough to neglect nonlinear effects; pressure and velocity measurements are compared using linear wave theory.

The methodology for comparing the AD current meter and pressure array data is developed below and is applied to the observations in section 4. The basic AD current meter performance can be verified through a comparison of the directly measured (with  $P_{10}$ ) bottom pressure frequency spectrum  $E_b(f)$  and a prediction based on the AD velocity measurements. The horizontal and vertical orbital velocity components of surface gravity waves are 90° out of phase so that the cospectra of  $u$  and  $w$  and of  $v$  and  $w$  theoretically vanish. Hence it follows from the first term on the right-hand side of (2) (i.e., the unexpanded term) that the frequency spectra  $E_{X_+}(f)$  and  $E_{X_-}(f)$  of the  $X_+$  and  $X_-$  beam measurements, respectively, are both equal to the sum  $\frac{1}{2}[E_u(f) + E_w(f)]$  of the  $u$  and  $w$  frequency spectra, and  $E_{Y_+}(f)$  and  $E_{Y_-}(f)$  are both equal to  $\frac{1}{2}[E_v(f) + E_w(f)]$ . Thus, according to linear wave theory the sum of the velocity frequency spectra of all four beams is related to  $E_b(f)$  by

$$E_{X_+}(f) + E_{X_-}(f) + E_{Y_+}(f) + E_{Y_-}(f) = E_u(f) + E_v(f) + 2 E_w(f) = \left[ \frac{gk}{2\pi f} \right]^2 [1 + 3 \sinh^2(kD)] E_b(f) \quad (7)$$

Note that (7) (applied to the observations in section 4) is not based

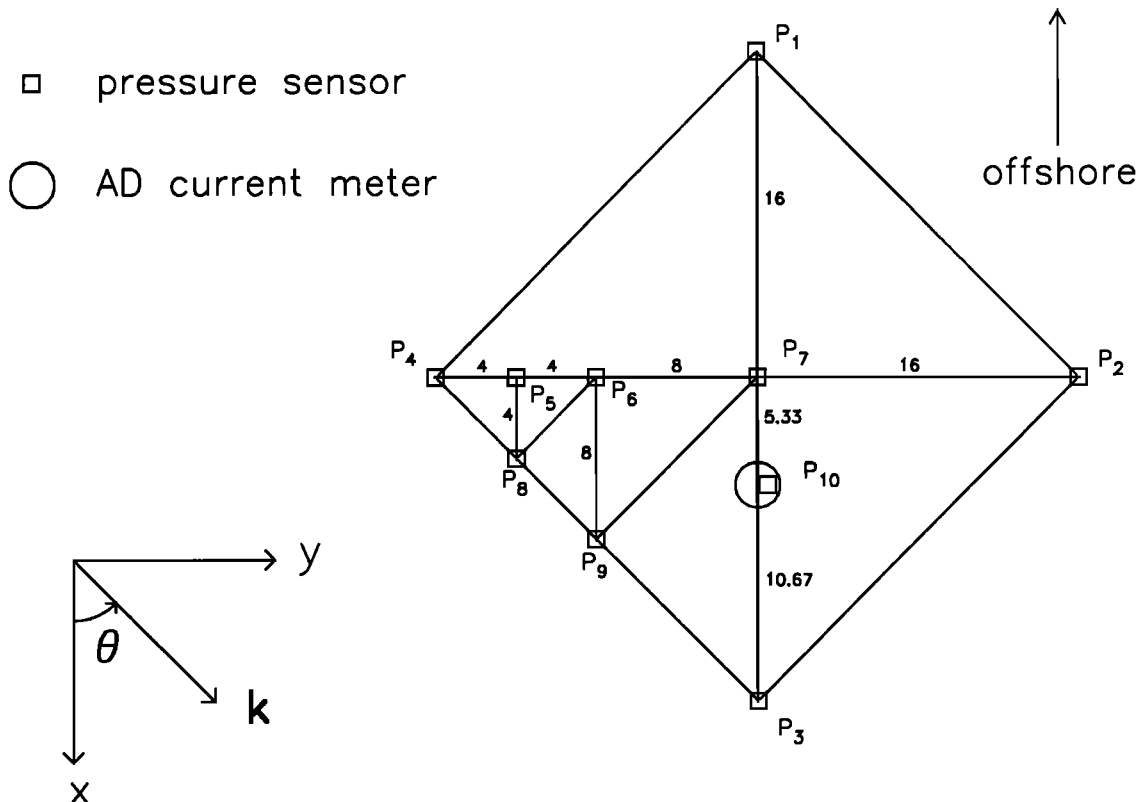


Fig. 2. Plan view of pressure sensor array geometry, AD current meter location, and analysis coordinate frame. Distances are given in m.

on a small  $kR$  expansion and thus holds for all wavelengths that are long compared to the dimensions of the sample volume, independent of the spatial separation of the sample volumes.

The cospectra  $C_{pp}$ ,  $C_{uu}$ ,  $C_{vv}$ ,  $C_{pu}$ ,  $C_{pv}$ , and  $C_{uv}$ , of pressure  $p$ , and horizontal velocity components  $u$  (cross-shore) and  $v$  (longshore), yield the lowest Fourier coefficients  $a_1$ ,  $b_1$ ,  $a_2$ , and  $b_2$  of the directional distribution  $S(\theta)$  (equation (1)), containing the dynamically important radiation stress components  $S_{xx}$ ,  $S_{yy}$ , and  $S_{xy}$ :

$$c_{pu}(f) \equiv \frac{C_{pu}(f)}{[C_{pp}(f)C_{uu}(f)]^{1/2}} = \frac{a_1}{(\frac{1}{2} + \frac{1}{2}a_2)^{1/2}} \quad (8a)$$

$$c_{pv}(f) \equiv \frac{C_{pv}(f)}{[C_{pp}(f)C_{vv}(f)]^{1/2}} = \frac{b_1}{(\frac{1}{2} - \frac{1}{2}a_2)^{1/2}} \quad (8b)$$

$$\frac{C_{uu}(f) - C_{vv}(f)}{C_{uu}(f) + C_{vv}(f)} = a_2 = \frac{S_{xx}(f) - S_{yy}(f)}{\rho g n(f) E_\eta(f)} \quad (8c)$$

$$\frac{2C_{uv}(f)}{C_{uu}(f) + C_{vv}(f)} = b_2 = \frac{2S_{xy}(f)}{\rho g n(f) E_\eta(f)} \quad (8d)$$

where  $\rho$  is the density of seawater,  $g$  is the acceleration of gravity,  $n$  is the ratio of group to phase velocity,  $E_\eta$  is the frequency spectral density of surface elevation, and the wave direction  $\theta$  is defined in Figure 2. Theoretically, the quadrature spectra of  $p$ ,  $u$ , and  $v$  are all identically zero.

The four directional parameters defined by (8) can be calculated from the cospectra of the AD beam differences and collocated pressure sensor  $P_{10}$  (with the assumptions of linear theory and small  $kR$ , equation (4)):

$$\frac{a_1}{(\frac{1}{2} + \frac{1}{2}a_2)^{1/2}} = \frac{C_{P_{10}X_{dY}}}{[C_{P_{10}P_{10}}C_{X_{dY}X_{dY}}]^{1/2}} + O(kR)^2 \quad (9a)$$

$$\frac{b_1}{(\frac{1}{2} - \frac{1}{2}a_2)^{1/2}} = \frac{C_{P_{10}Y_{dY}}}{[C_{P_{10}P_{10}}C_{Y_{dY}Y_{dY}}]^{1/2}} + O(kR)^2 \quad (9b)$$

$$a_2 = \frac{C_{X_{dY}X_{dY}} - C_{Y_{dY}Y_{dY}}}{C_{X_{dY}X_{dY}} + C_{Y_{dY}Y_{dY}}} + O(kR)^2 \quad (9c)$$

$$b_2 = \frac{2C_{X_{dY}Y_{dY}}}{C_{X_{dY}X_{dY}} + C_{Y_{dY}Y_{dY}}} + O(kR)^2 \quad (9d)$$

For the frequency range considered in the comparisons in section 4 (0.04–0.30 Hz), the  $O(kR)^2$  velocity curvature bias errors in (9) are negligibly small (equation (4)).

The pressure transducer array forms the basis for verification of acoustic Doppler directional wave data (equation (9)). The nine sensors in the array were mounted on the seafloor by divers with a placement accuracy of about 5 cm. A compact array geometry

was chosen with equally spaced lags both along the array axes and along the array diagonals (45 degrees relative to the array axes, Figure 2) that can provide estimates of  $a_1$ ,  $b_1$ ,  $a_2$ , and  $b_2$  (equations (1) and (8)) with very small bias. The pressure array data were analyzed with an estimation technique [Herbers and Guza, 1989] for slope arrays (four pressure sensors arranged in a square) with dimension  $L$  which is small compared to the surface wavelength. For  $kL < 1.5$ , the Fourier coefficients  $a_1$ ,  $b_1$ ,  $a_2$ , and  $b_2$  can be expressed to a high degree of accuracy as linear sums of normalized slope array cross spectra [Herbers and Guza, 1989]. The slope array method, based on an expansion for small  $kL$ , does not necessarily require a square array geometry. Various combinations of four sensors each in Figure 2 have the same coarray as a slope array and therefore can also be analyzed with the same estimators. For  $kL > 1.5$ , bias errors in the estimates increase rapidly due to contributions from neglected higher-order terms in the expansion. On the other hand, for very small  $kL$ , the coefficients of the estimators (proportional to  $(kL)^{-1}$  for  $a_1$  and  $b_1$  and to  $(kL)^{-2}$  for  $a_2$  and  $b_2$ ) become large, and the estimates are sensitive to instrument noise. This small  $kL$  limit is not known a priori because the statistics of instrument and data acquisition system noise are poorly understood.

A slope array of fixed dimension  $L$  can thus provide accurate pitch-and-roll type information only for a limited range of wavelengths. However, by combining subarrays with various  $L$ , the accuracy of the AD current meter can be verified for a wide frequency range. Estimates of the directional moments given by (8) were computed for (slope) subarrays  $P_4-P_5-P_6-P_8$ ,  $P_4-P_6-P_7-P_9$ , and  $P_2-P_3-P_4-P_7$  ( $L = 4, 8$ , and  $16$  m, respectively; Figure 2) in their "optimal" range  $0.5 < kL < 1.5$  where the theoretical bias is small and estimates are not very sensitive to instrument noise. Together these estimates span the sea and swell frequency range (0.04–0.30 Hz) considered in the intercomparisons. The lower  $kL = 0.5$  limit was determined empirically by comparing subarrays. Estimates using all other possible subarrays, with overlapping optimal  $kL$  ranges, do not differ significantly from the estimates presented in section 4, and they confirm that errors in the ground truth pressure array data are indeed small.

#### 4. COMPARISONS

In this section measurements from the acoustic Doppler system and pressure array are compared using linear theory, for 0.04 Hz  $< f < 0.30$  Hz, typically spanning the range of frequencies of sea and swell waves in the Pacific Ocean. Figure 3 shows comparisons of the measured bottom pressure spectrum  $E_{b,meas}(f)$ , obtained from sensor  $P_{10}$  with a (small) linear theory depth correction for the height of the transducer above the seabed ( $\approx 0.5$  m), and the bottom pressure spectrum  $E_{b,pred}(f)$ , predicted from the AD velocity measurements with (7). The gain function  $G(f)$  defined as

$$G(f) \equiv \left[ \frac{E_{b,pred}(f)}{E_{b,meas}(f)} \right]^{1/2} \quad (10)$$

is shown in Figure 4. The agreement is generally excellent across the wide frequency range considered here, except for low frequencies ( $f < 0.08$  Hz) where measured and predicted spectra sometimes diverge. Inspection of the raw acoustic data suggests that these discrepancies are due to contamination of the received sound by reflections from the sea surface. On one occasion (Figure 3a) the predicted and measured spectra agree also very well at low frequencies, possibly because the signal-to-noise ratio is enhanced by the presence of a 0.05-Hz swell peak.

In all four cases  $G(f) = 1 \pm 0.05$  in a frequency range (0.08–0.30 Hz) that extends to about twice the spectral peak frequency  $f_p$ , where energy density levels are 2 orders of magnitude smaller than the spectral peak level. This high level of agreement

is remarkable considering the weak root-mean-square orbital wave velocities measured by the acoustic Doppler beams ( $O(10 \text{ cm/s})$ ) and suggests that instrument noise levels of the present (still far from optimal) AD system are very weak. The

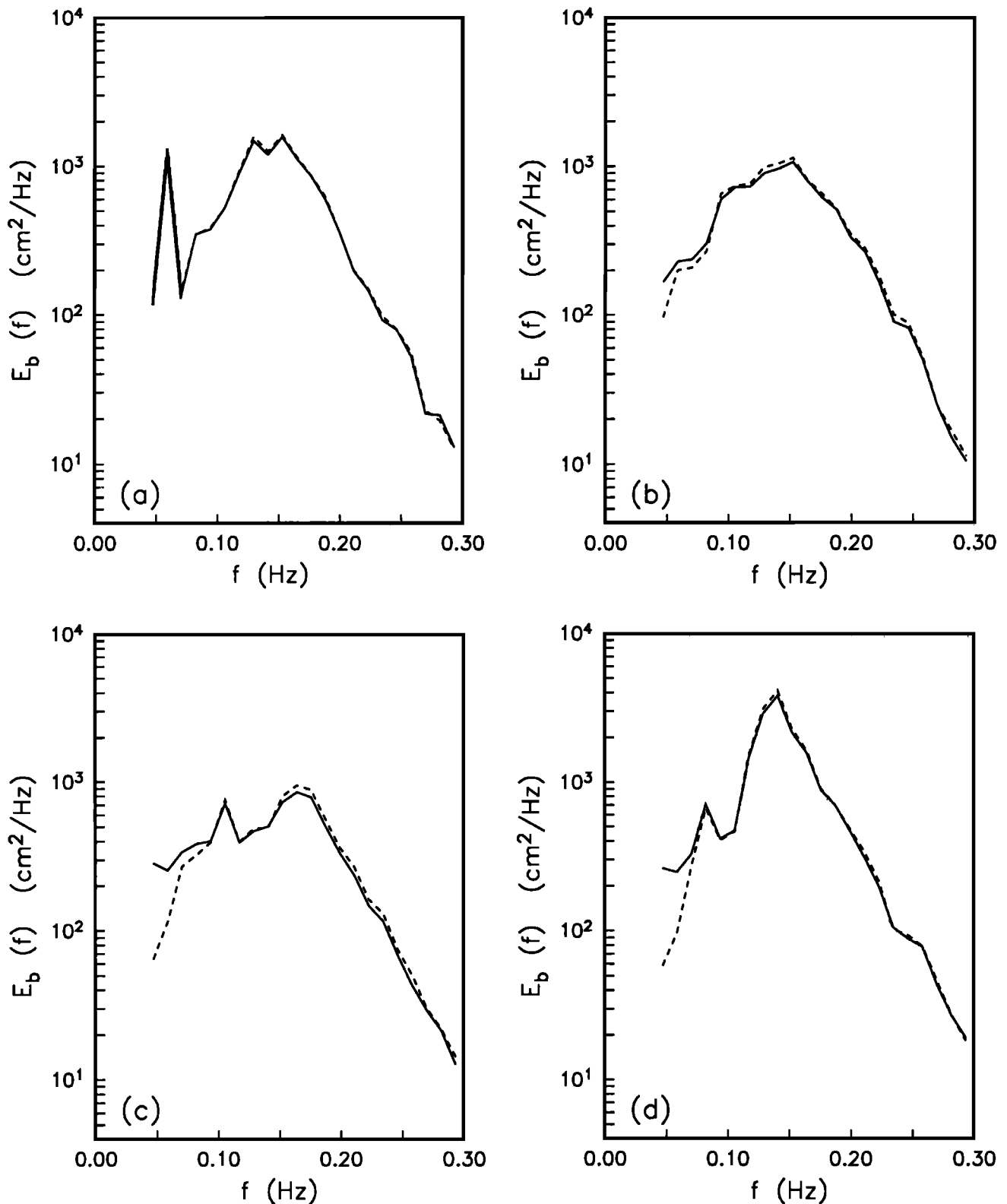


Fig. 3. Comparison of bottom pressure spectra predicted from the acoustic Doppler velocity measurements ( $E_{b,pred}(f)$ , solid curve) and directly measured ( $E_{b,meas}(f)$ , dashed curve) on (a) August 30 (43-min records, 60 degrees of freedom), (b) September 7 (56-min records, 78 degrees of freedom), (c) September 8 (90-min records, 126 degrees of freedom), and (d) September 11 (102-min records, 144 degrees of freedom), 1989. The root-mean-square bottom pressure fluctuations for the August 30 and September 7, 8, and 11 data runs are 11.6, 10.2, 9.5, and 14.2 cm, respectively.

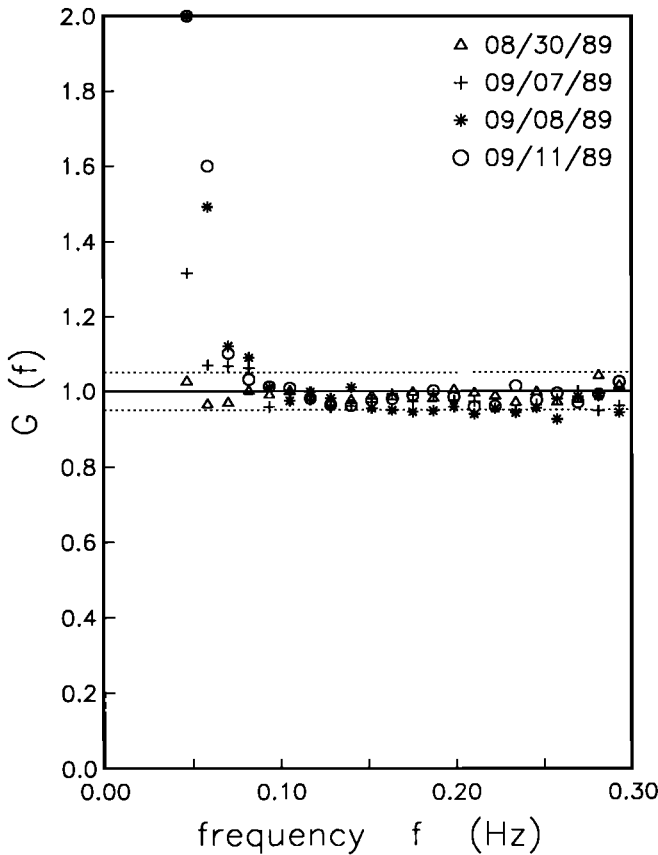


Fig. 4. Estimates of the normalized gain function  $G(f)$ , between velocity and pressure measurements, defined by (10). The dotted lines indicate the 5% error levels 0.95 and 1.05. Values greater than 2.0 are set equal to 2.0 for display purposes.

total gain  $G_{tot}$ ,

$$G_{tot} \equiv \left[ \frac{\int_{0.04\text{Hz}}^{0.30\text{Hz}} df E_{b, \text{pred}}(f)}{\int_{0.04\text{Hz}}^{0.30\text{Hz}} df E_{b, \text{meas}}(f)} \right]^{1/2} \quad (11)$$

for the August 30 and September 7, 8, and 11 data runs is 0.98, 0.98, 1.00, and 0.99, respectively. These gain errors are within the calibration uncertainty of the pressure sensor and confirm that the AD velocity measurements are unbiased.

Figure 5 shows a comparison of the normalized cospectra,  $c_{pv}(f)$  and  $c_{pu}(f)$  (equations (8a) and (8b)), obtained from pressure sensor  $P_{10}$  and the AD current meter with (9a) and (9b) and predictions extracted from the pressure array data [Herbers and Guza, 1989, equation (9)]. The relative orientation of the pressure array and AD current meter in the horizontal plane was only crudely known, and a constant  $5^\circ$  rotation between them (which improved the comparisons below) was assumed for all analysis. Since the  $p-u$  and  $p-v$  quadrature spectra theoretically vanish for surface gravity waves, the  $p-u$  and  $p-v$  coherencies are equal to  $|c_{pu}|$  and  $|c_{pv}|$ , respectively (assuming that turbulence contributions to the velocity measurements are negligible at sea and swell frequencies; Figures 3 and 4). These coherencies are equal to 1 for unidirectional waves ( $a_1^2 = \frac{1}{2} + \frac{1}{2} a_2$  and  $b_1^2 = \frac{1}{2} - \frac{1}{2} a_2$ ) but are generally reduced by the finite width of  $S(\theta)$  ( $a_1^2 < \frac{1}{2} + \frac{1}{2} a_2$

and  $b_1^2 < \frac{1}{2} - \frac{1}{2} a_2$ , equations (1) and (8) [Kitaigorodskii et al., 1983]). On all four occasions, the measured and predicted  $c_{pu}$  are very close to 1 (Figure 5). Only a small decrease in the coherence between pressure and the cross-shore velocity component  $u$  due to directional spreading is expected since angles of incidence of long-wavelength swell are reduced by refraction, the fetch for wind waves with large oblique angles of incidence is limited at this site, and reflection is weak from the gently sloping beach. On the other hand, in all cases the absolute value of both measured and predicted  $c_{pv}$  is much smaller than 1, indicating that the coherence of pressure and the longshore velocity  $v$  is greatly reduced by directional spreading (Figure 5), with significant energy arriving from both offshore quadrants (i.e., both  $\theta < 0$  and  $\theta > 0$ , Figure 2). On all four days, the measured  $c_{pu}$  and  $c_{pv}$  are in excellent agreement with the predictions from the pressure array data across the entire frequency range (0.04–0.30 Hz) considered in the comparisons (Figure 5). The quadrature spectra (not shown) between  $P_{10}$  and  $X_{dir}$  and between  $P_{10}$  and  $Y_{dir}$  are within the expected statistical scatter about zero, also consistent with theory.

Estimates of  $a_2$  and  $b_2$  (the normalized wave radiation stresses, equations (8c) and (8d)) obtained from the AD current meter (equations (9c) and (9d)) and from the pressure array data [Herbers and Guza, 1989, equation (9)] are compared in Figure 6. The results generally show good agreement on all four days. On September 7, 8, and 11 (Figures 6b, 6c and 6d), the lowest-frequency bands show discrepancies between AD current meter estimates and pressure array estimates, which are possibly due to contamination of the acoustic Doppler data by reflections from the sea surface (Figure 3). At the spectral peak the agreement is excellent on all four days, while at higher frequencies the velocity- and pressure-based estimates agree well on August 30 and September 11 (Figures 6a and 6d) but diverge somewhat on the other two days (Figures 6b and 6c).

Figures 5 and 6 clearly confirm that the present AD current meter, together with a pressure sensor, can provide low-resolution directional wave data comparable to pitch-and-roll type measurement systems. Higher-resolution directional wave data (i.e.,  $a_3$ ,  $b_3$ , and  $a_4$ ) can in principal be obtained from the AD current meter if both the beam differences (i.e.,  $u$  and  $v$ , equations (3) and (4)) and the beam sums (i.e.,  $u_x$  and  $v_y$ , equations (5) and (6)) are included in the analysis. Because of the small separation of the AD sample volumes, the measured velocity gradients  $u_x$  and  $v_y$  ( $O(kR)$ , equation (6)) are expected to be very sensitive to instrument noise and other sources of errors (e.g., a misalignment of the instrument in the horizontal plane, turbulence), and the present system is clearly not optimal for obtaining higher-order directional wave data. Nevertheless, it is of interest to examine the accuracy of the  $X_{sum}$  and  $Y_{sum}$  measurements to assess the limitations of the present system. The cospectra of  $X_{sum}$  and  $Y_{sum}$  can be combined to predict the bottom pressure spectrum  $E_b(f)$  (equation (6)):

$$H(f) \equiv \frac{[C_{X_{sum}X_{sum}}(f) + 2C_{X_{sum}Y_{sum}}(f) + C_{Y_{sum}Y_{sum}}(f)]^{1/2} 2\pi f}{[E_b(f)]^{1/2} |(2 - \frac{1}{2}(kR)^2) \sinh(kD) - kR \cosh(kD)| gk} = 1 + O(kR)^3 \quad (12)$$

where  $H(f)$  is the gain ratio between  $X_{sum} + Y_{sum}$  and bottom pressure, normalized by the theoretical value for linear surface gravity waves. The  $\sinh(kD)$  term in (12) contains the  $w$ ,  $w_{xx}$ , and  $w_{yy}$  contributions to  $H(f)$  while the  $\cosh(kD)$  term contains the  $u_x$  and  $v_y$  contributions (equations (5) and (6)). For the frequency range (0.04–0.30 Hz), beam locations, and water depth

considered here, the beam sum measurements are dominated by  $w$  with  $u_x$  and  $v_y$  contributing only approximately 20% to  $H(f)$ . The  $O(kR)^3$  bias in (12) is negligibly small for  $f < 0.3$  Hz. Figure 7 shows estimates of  $H(f)$  with  $E_b(f)$  calculated from colocated

pressure sensor  $P_{10}$ , as in Figures 3 and 4. For  $f > 0.1$  Hz, Figure 7 shows good agreement between what is essentially the vertical velocity and pressure measurements, with  $H(f)$  within  $1 \pm 0.1$  on all days, except for the September 8 data run that shows slightly

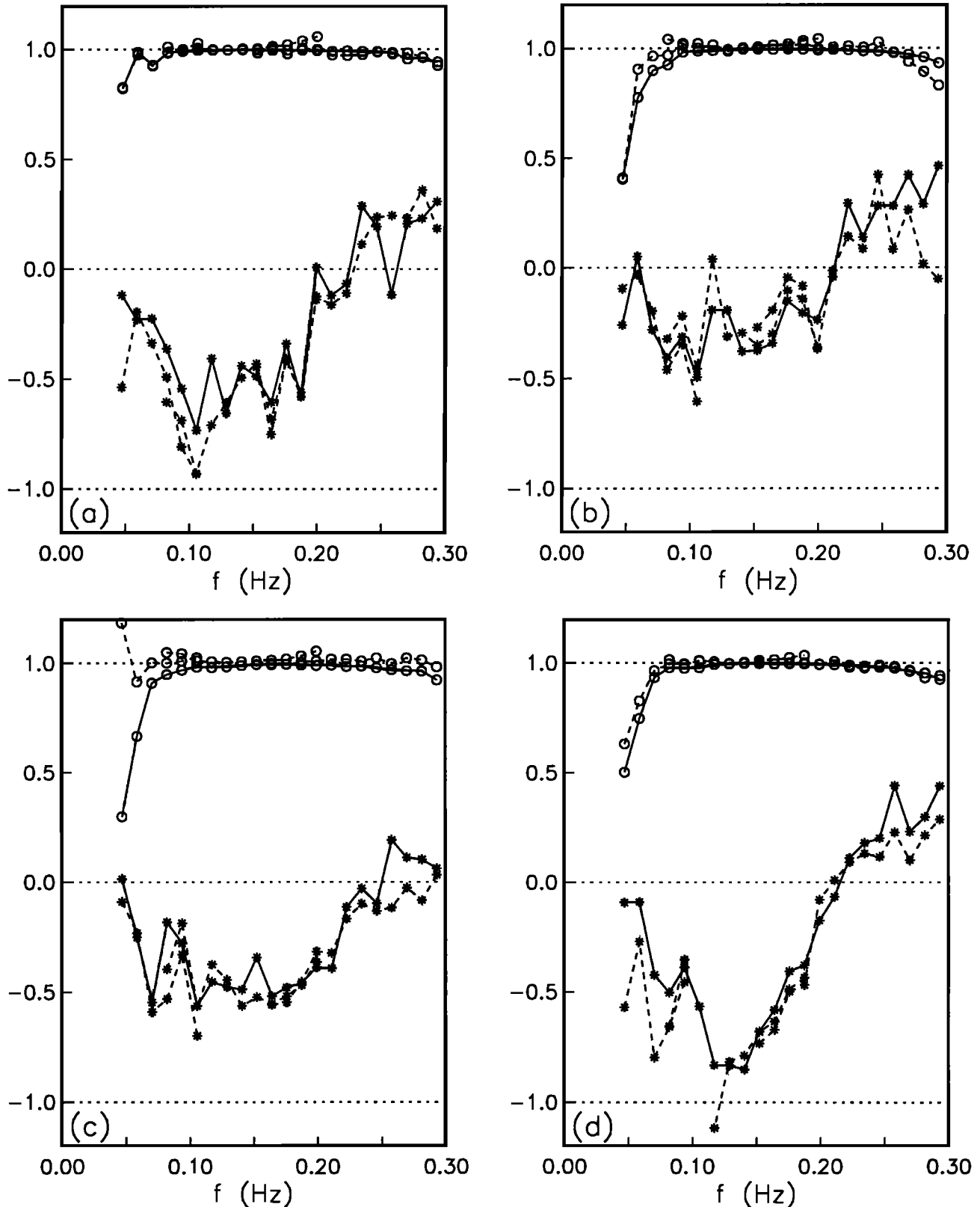


Fig. 5. Normalized cospectra  $c_{pu}(f)$  (circles) and  $c_{pv}(f)$  (asterisks) between pressure and velocity, obtained directly from the AD current meter and colocated pressure sensor  $P_{10}$  (solid curves) and theoretically predicted from the pressure array data (dashed curves are predictions from three different subarrays). Measured and predicted cospectra are compared on (a) August 30, (b) September 7, (c) September 8, and (d) September 11, 1989. Record lengths and degrees of freedom are the same as in Figure 3.

larger errors ( $H(f) = 1 \pm 0.15$ ). At lower frequencies the errors in these  $H(f)$  estimates are larger than errors in the analogous ratio  $G(f)$  (equations (7) and (10)) based on horizontal velocities (compare Figures 4 and 7). This is not surprising since the measured

vertical velocities at swell frequencies are about an order of magnitude smaller than the horizontal velocities, and measurement errors evident in Figures 3 and 4 are relatively more important in  $H(f)$  estimates.

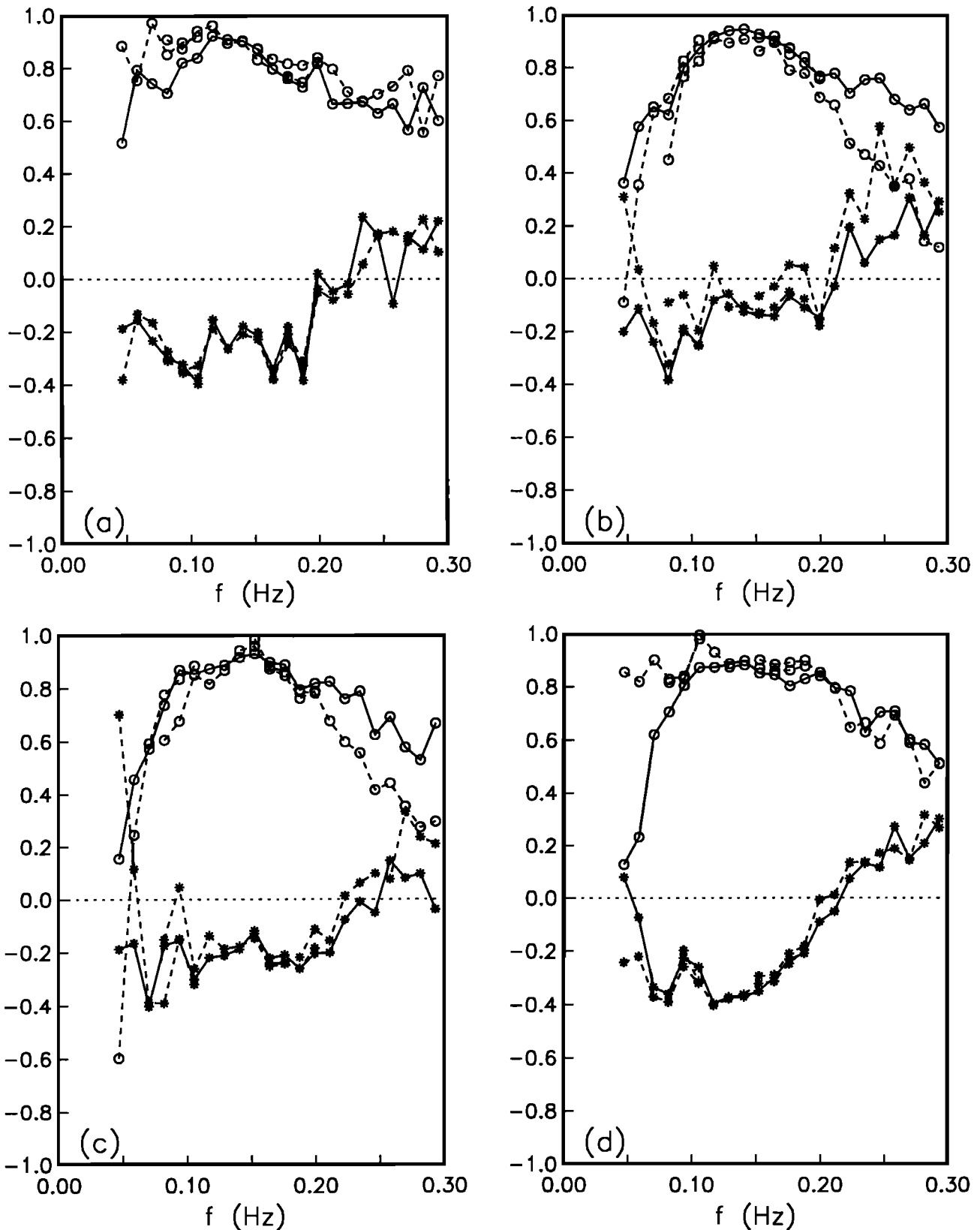


Fig. 6. Comparison of normalized wave radiation stresses  $a_2(f)$  (circles) and  $b_2(f)$  (asterisks), estimated from the AD current meter (solid curves) and from the pressure array data (dashed curves correspond to three different subarrays), on (a) August 30, (b) September 7, (c) September 8, and (d) September 11, 1989. Record lengths and degrees of freedom are the same as in Figure 3.

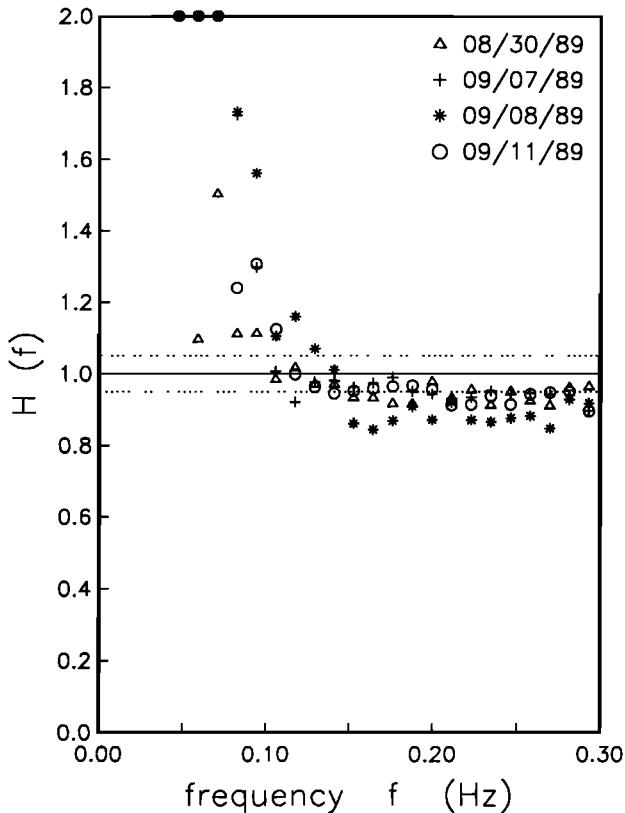


Fig. 7. Estimates of the normalized gain function  $H(f)$ , between velocity and pressure measurements, defined by (12). The dotted lines indicate the 5% error levels 0.95 and 1.05. Values greater than 2.0 are set equal to 2.0 for display purposes.

## 5. DISCUSSION

The overall level of agreement between the frequency spectra of pressure and AD velocity measurements (Figure 4) is somewhat better than the gain errors ( $G(f) = 1 \pm 0.1$ ) reported by *Guza and Thornton* [1980] and *Guza et al.* [1988], based on comparisons of EM current meters and pressure sensors in a similar environment, but covering a much wider range of wave conditions. *Battjes and Van Heteren* [1984] also report gain errors  $G(f) = 1 \pm 0.1$  near the spectral peak  $f_p$ , but larger discrepancies at frequencies  $f > 2f_p$ , based on extensive comparisons of an ATT current meter and a surface height gauge in the North Sea in 17-m depth. *Battjes and Van Heteren* note that it is possible that the disagreement with linear theory at high frequencies is due to measurement errors, and they question numerous earlier investigations that attributed observed anomalies in the transfer function between velocity and surface height/pressure measurements to turbulence and wave nonlinearity. A particular cause for concern with in situ EM and ATT current meters is the uncertainty in their response associated with the flow disturbance around the probe. These problems do not arise with the present nonobtrusive AD current meter, and measurements of second-order velocities are thus less controversial. The close quantitative agreement with linear theory, of velocity and pressure measurements of relatively small amplitude waves (Figures 3 and 4), suggests that the AD technique is potentially accurate enough for measuring turbulence and wave nonlinearity in more energetic seas. However, the beam geometry of the present AD instrument is not well suited to turbulence measurements. Since length scales of turbulence may not be large compared to the separation of the sample volumes, tur-

bulence contributions to estimates of  $u$ ,  $v$  and  $w$  based on the AD beam sums and differences (equations (4) and (6)) may be aliased (note that the comparisons in Figures 3 and 4 are based on (7), valid for all wavelengths that are long compared to the dimensions of the sample volume, Figure 1b). Nonlinear wave contributions to the flow field (i.e., forced components that do not obey a dispersion relation) may have very short wavelengths, but they are strongly attenuated at depths below the sea surface that exceed their wavelength [e.g., *Hasselmann*, 1962]. Hence, if the depth of submergence of the AD sample volumes is much larger than their horizontal separation ( $h - D \gg R$  with  $h$  the water depth), then the components  $u$  and  $v$  of nonlinear surface waves can in principle be extracted from the beam differences (equation (3)) and (for  $D \gg R$ , Figure 1a)  $w$  can be obtained from the beam sums (equation (5)).

In addition to providing the lowest Fourier coefficients  $a_1$ ,  $b_1$ ,  $a_2$ , and  $b_2$  of the directional distribution  $S(\theta)$  (equation (8)), cross spectra of pressure (or surface height) and velocity measurements are frequently used to separate orbital wave velocities and turbulence (i.e., motions not associated with wave surface excursions) in wind waves [e.g., *Kitaigorodskii et al.*, 1983; *Terray and Bliven*, 1985; *Cheung and Street*, 1988; *Agrawal et al.*, 1988]. These so-called "linear filtration" techniques are based on the assumption that the coherence between wave-induced velocity and pressure is 1 and any observed coherence reduction is due to turbulence. Although the coherence between  $p$  and the vertical velocity component  $w$  is not influenced by  $S(\theta)$ , *Kitaigorodskii et al.* [1983] note that a fundamental difficulty with applying this technique to the horizontal velocity components  $u$  and  $v$  is the unknown reduction of the  $p-u$  and  $p-v$  coherencies due to directional spreading of the surface waves (equations (8a) and (8b)), which would be falsely attributed to turbulence contributions to the flow field, and they suggest that the turbulence spectra that they estimated from wind wave observations in Lake Ontario may have significant errors due to this effect. The large observed and predicted reductions of the coherence between  $p$  and the longshore velocity component  $v$  (Figure 5) illustrate that directional spreading effects on natural wind waves can cause large errors in turbulence estimates based on linear filtration techniques using pressure or surface elevation measurements. However, the coherence of  $p_x$  and  $u$  ( $p$ , and  $v$ ) is unity for linear waves independent of  $S(\theta)$ , so this bias can be avoided if pressure gradients are measured with a compact array of pressure sensors (or surface slopes with a compact array of surface height gauges). The separation of turbulence and wave-induced velocities can thus be based on the cross spectra of  $p_x$  and  $u$  ( $p$ , and  $v$ ).

The comparisons of pressure and AD velocities based on the beam sums (equation (12), Figure 7) suggest that at swell frequencies ( $f < 0.08$  Hz) the separation of sample volumes in the present system is too small to provide meaningful estimates of  $a_3$ ,  $b_3$ , and  $a_4$ , and the sample volumes are too close to the seafloor to measure  $w$ . Further improvements of the instrument (i.e., reduction of surface reflection effects) are expected to improve the measurement of  $w$  and hence to yield  $H(f)$  estimates closer to the theoretical value of 1. However, the ratio between the velocity differences  $u_x R$  and  $v_x R$  and the velocities  $u$  and  $v$  varies between only 2% for 0.04-Hz swell to 25% for 0.3-Hz seas, for the present beam configuration. Hence, the sensitivity to measurement errors for swell is such that a small misalignment of the AD current meter out of the horizontal plane may contribute relatively large errors to higher-order directional information that depends on the velocity gradients  $u_x$  and  $v_x$ . A larger separation of the sample volumes will reduce this sensitivity but will also increase bias

errors in estimates of  $a_n$  and  $b_n$ . This increase in bias may be reduced with improved estimators based on (4) and (6) (analogous to *Herbers and Guza* [1989]), but for  $kR > 1$  the AD system simply lacks the necessary directional information. Results of the intercomparison study suggest that the acoustic Doppler velocity measurements are sufficiently accurate that a slightly modified AD system with  $R$  increased to about 2–3 m may yield stable, approximately unbiased estimates of  $a_1$ ,  $b_1$ ,  $a_2$ ,  $b_2$ ,  $a_3$ ,  $b_3$ , and  $a_4$  at sea and swell frequencies.

The present intercomparison study spans a very limited range of conditions with relatively small wind waves. Although some whitecapping may have occurred during these observations, the AD velocity measurements were taken at a depth below the sea surface where bubble concentrations induced by wave breaking are expected to be very small. It is possible that close to the sea surface under energetic (breaking) wind waves AD velocity measurements are degraded by air entrainment. Work in progress examines the limitations of the AD technique through comparisons of velocity and pressure measurements of surface waves at various elevations below the sea surface for a wider variety of conditions. Preliminary results in 7 m depth with the sample volumes about 2.5 m above the seafloor suggest that the instrument can function well in at least moderately energetic waves, with root-mean-square orbital velocities a few times larger than reported here.

## 6. CONCLUSIONS

A field verification is presented of nearshore surface gravity wave measurements obtained with an acoustic Doppler (AD) current meter. The instrument, mounted on the seafloor, contains four beams, inclined 45° from vertical, that measure the along-beam velocity at a single range of 1 m (Figure 1). By expanding the velocity measurements about the instrument center, and assuming linear theory, it is shown that the lowest four Fourier coefficients  $a_1$ ,  $b_1$ ,  $a_2$ , and  $b_2$  of the directional distribution  $S(\theta)$  (equation (1)) can be expressed to a high degree of accuracy in terms of the cospectra of the AD current meter and a colocated pressure sensor. Thus the present AD instrument and a pressure sensor form a PUV system providing directional information comparable to a pitch-and-roll buoy. Unbiased estimates of the higher-order Fourier coefficients  $a_3$ ,  $b_3$ , and  $a_4$  can in principal also be extracted from the AD data, but for the limited range (1 m) of the present instrument, these estimates are expected to be sensitive to measurement errors.

The AD current meter was field tested in the summer of 1989 in 7-m depth near the end of the Scripps Institution of Oceanography pier, with the objectives of examining the accuracy of the velocity measurements and the feasibility of obtaining directional wave measurements with a compact relatively easily deployable device. A pressure sensor was positioned as close as possible to the AD current meter so that velocity and pressure measurements could be compared using linear theory. The AD current meter and this colocated pressure sensor together form a PUV system that was embedded in an array of pressure sensors for an intercomparison of directional wave information (Figure 2). Unbiased estimates of  $a_1$ ,  $b_1$ ,  $a_2$ , and  $b_2$  were extracted from the pressure array data with the method of *Herbers and Guza* [1989]. Pressure and velocity measurements are compared, in the sea and swell frequency range 0.04–0.30 Hz, on four occasions with waves small enough that nonlinear effects are expected to be negligible.

Intercomparisons of bottom pressure spectra, directly measured and predicted from the AD velocity measurements assuming

linear theory, show excellent agreement (Figures 3 and 4). Differences between predicted and measured pressure spectra are generally less than 10% (i.e., gain errors of less than 5%), and the predicted and measured pressure total variances (over the frequency range 0.04–0.30 Hz) differ by only a few percent. The overall agreement is somewhat better than previously reported results, comparing pressure sensors and electromagnetic current meters [*Guza and Thornton*, 1980; *Guza et al.*, 1988] and comparing a surface height gauge and an acoustic travel time current meter ([*Battjes and Van Heteren* [1984], in a different environment), although it is noted that these earlier studies span a much wider range of wave conditions.

It is well known that carefully calibrated electromagnetic and acoustic travel time current meters can function well, but measurements of second-order (i.e., turbulence and wave nonlinearity) velocities are fundamentally difficult to obtain with these obtrusive in situ instruments because of uncertainties in their dynamic response, which may increase in field deployments due to biofouling of the probe. The present study illustrates the important advantage of a nonobtrusive instrument with a response that is well understood and therefore does not require a calibration. Although AD velocity measurements may not be feasible in every environment and results of the field test suggest further modifications of the present instrument (i.e., reduce the effect of reflections from the sea surface), the comparisons demonstrate that highly accurate wave measurements can be obtained with a relatively simple AD instrument. Acoustic Doppler techniques may be useful in field studies of the generally weak contributions of turbulence and wave nonlinearity to the velocity field.

Cross spectra between pressure  $p$  and horizontal velocity components  $u$  and  $v$  are compared to linear wave theory predictions obtained from the pressure array data. Observed and predicted normalized cospectra (equation (8), the quadrature spectra theoretically vanish) are in excellent agreement across the entire sea and swell frequency range (Figure 5). On all four days the coherence between  $p$  and the cross-shore component  $u$  is high ( $\approx 1$  at all frequencies), but the coherence between  $p$  and the longshore component  $v$  is significantly reduced ( $\approx 0$  at some frequencies) due to the directional spread of the wave field. Pressure-velocity cross spectra are frequently used to separate turbulence from the wave orbital motion assuming that the coherence between wave-induced velocities and pressure is equal to 1. A (potentially large) bias in turbulence estimates, due to wave directional spreading effects, may be avoided if pressure gradients  $p_x$  and  $p_y$  are measured with a compact array of pressure sensors [*Herbers and Guza*, 1989], and the separation of turbulence and wave-induced velocities is based on the cross spectra of  $p_x$  and  $u$  ( $p_y$  and  $v$ ) rather than  $p$  and  $u$  ( $p$  and  $v$ ).

Wave radiation stresses are important to nearshore process studies and are routinely collected at various coastal sites. A comparison of normalized radiation stress estimates ( $a_2$  and  $b_2$ , equation (8)) obtained from the AD current meter and estimates extracted from the pressure sensor array show good agreement (Figure 6). The results of this intercomparison study show that the present AD current meter together with a colocated pressure sensor can provide accurate pitch-and-roll type directional wave data.

*Acknowledgments.* The initial phases of this work, including development of the sensor, result from research sponsored in part by NOAA, National Sea Grant College Program, Department of Commerce, under grant NA85AA-D-SG140, project R/OE-4, through the California Sea Grant College Program, and in part by the California State Resources Agency. The U.S. Government is authorized to reproduce and distribute for governmental purposes. The analysis was completed with support

from the Coastal Sciences Branch of the Office of Naval Research, grant N00014-89-J-1055. The staff of the Center for Coastal Studies (Scripps Institution of Oceanography) installed and maintained the instruments and data acquisition systems. We thank M. H. Freilich for helpful discussions and the anonymous reviewers for useful suggestions. This manuscript was prepared while T.H.C.H. and R.T.G. were visiting the CERC Field Research Facility in Duck, NC. We thank the FRF staff for their hospitality.

## REFERENCES

- Agrawal, Y., D. G. Aubrey, and F. Dias, Field observations of the coastal bottom boundary layer under surface gravity waves, Proceedings 4th International Symposium on Applications of Laser Anemometry in Fluid Mechanics, Lisbon, Portugal, July 11–14, 1988, *Pap. 4.7*, Inst. Super. Tech., Lisbon, Portugal, 1988.
- Allender, J., T. Audunson, S. F. Barstow, S. Bjerken, H. E. Krogstad, P. Steinbakke, L. Vartdal, L. E. Borgman, and C. Graham, The WADIC project: A comprehensive field evaluation of directional wave instrumentation, *Ocean Eng.*, *16*(5/6), 505–536, 1989.
- Battjes, J. A., and J. Van Heteren, Verification of linear theory for particle velocities in wind waves based on field measurements, *Appl. Ocean Res.*, *6*(4), 187–196, 1984.
- Bodge, K. R., and R. G. Dean, Wave measurements with differential pressure gauges, in *Proceedings 19th International Conference Coastal Engineering*, edited by B. L. Edge, pp. 755–769, American Society of Civil Engineers, New York, 1984.
- Bowden, K. F., and R. A. White, Measurements of the orbital velocities of sea waves and their use in determining the directional spectrum, *Geophys. J. R. Astron. Soc.*, *12*, 33–54, 1966.
- Cartwright, D. E., and N. D. Smith, Buoy techniques for obtaining directional wave spectra, in *Buoy Technology*, pp. 112–121, Marine Technological Society, Washington, DC, 1964.
- Cheung, T. K., and R. L. Street, The turbulent layer in the water at an air-water interface, *J. Fluid Mech.*, *194*, 133–151, 1988.
- Derks, H., and M. J. F. Stive, Field investigations in the TOW study programme for coastal sediment transport in The Netherlands, in *Proceedings 19th International Conference Coastal Engineering*, edited by B. L. Edge, pp. 1830–1845, American Society of Civil Engineers, New York, 1984.
- Grosskopf, W. G., D. G. Aubrey, M. G. Mattie, and M. Mathiesen, Field intercomparison of nearshore directional wave sensors, *IEEE J. Oceanic Eng.*, *OE-8*(4), 254–271, 1983.
- Guza, R. T., and E. B. Thornton, Local and shoaled comparisons of sea surface elevations, pressures, and velocities, *J. Geophys. Res.*, *85*(C3), 1524–1530, 1980.
- Guza, R. T., M. C. Clifton, and F. Rezvani, Field intercomparisons of electromagnetic current meters, *J. Geophys. Res.*, *93*(C2), 9302–9314, 1988.
- Hasselmann, K., On the non-linear energy transfer in a gravity-wave spectrum, 1, General theory, *J. Fluid Mech.*, *12*, 481–500, 1962.
- Herbers, T. H. C., and R. T. Guza, Estimation of wave radiation stresses from slope array data, *J. Geophys. Res.*, *94*(C2), 2099–2104, 1989.
- Herbers, T. H. C., and R. T. Guza, Estimation of directional wave spectra from multicomponent observations, *J. Phys. Oceanogr.*, *20*(11), 1703–1724, 1990.
- Higgins, A. L., R. J. Seymour, and S. S. Pawka, A compact representation of ocean wave directionality, *Appl. Ocean Res.*, *3*, 105–112, 1981.
- Kitaigorodskii, S. A., M. A. Donelan, J. L. Lumley, and E. A. Terray, Wave-turbulence interactions in the upper ocean, II, Statistical characteristics of wave and turbulent components of the random velocity field in the marine surface layer, *J. Phys. Oceanogr.*, *13*, 1988–1999, 1983.
- Krogstad, H. E., R. L. Gordon, and M. C. Miller, High-resolution directional wave spectra from horizontally mounted acoustic Doppler current meters, *J. Atmos. Oceanic Technology*, *5*, 340–352, 1988.
- Lhermitte, R., Water velocity and turbulence measurements by coherent Doppler sonar, in *Oceans 85*, pp. 1159–1164, Institute of Electrical and Electronics Engineers, New York, 1985.
- Longuet-Higgins, M. S., and R. W. Stewart, Radiation stress and mass transport in surface gravity waves with application to 'surf beats', *J. Fluid Mech.*, *13*, 481–504, 1962.
- Longuet-Higgins, M. S., D. E. Cartwright, and N. D. Smith, Observations of the directional spectrum of sea waves using the motions of a floating buoy, in *Ocean Wave Spectra*, pp. 111–136, Prentice-Hall, Englewood Cliffs, N. J., 1963.
- Lowe, R. L., and R. T. Guza, Field test of Doppler acoustic directional wave sensor, *Rep. R/OE-4*, 9 pp., Calif. Sea Grant Coll. Program, University of California, La Jolla, 1990.
- Mitsuyasu, H., F. Tasai, T. Suhara, S. Mizuno, M. Ohkuso, T. Honda, and K. Rikishi, Observations of the directional spectrum of ocean waves using a cloverleaf buoy, *J. Phys. Oceanogr.*, *5*, 750–758, 1975.
- Nagata, Y., The statistical properties of orbital wave motions and their application for the measurement of directional wave spectra, *J. Oceanogr. Soc. Jpn.*, *19*, 169–181, 1964.
- Pawka, S. S., Island shadows in wave directional spectra, *J. Geophys. Res.*, *88*(C4), 2579–2591, 1983.
- Pinkel, R., and J. A. Smith, Open ocean surface wave measurements using Doppler sonar, *J. Geophys. Res.*, *92*, 12,967–12,973, 1987.
- Seymour, R. J., M. H. Sessions, and D. Castel, Automated remote recording and analysis of coastal data, *J. Waterw. Port Coastal Ocean Div. Am. Soc. Civ. Eng.*, *111*, 388–400, 1985.
- Simpson, J. H., Observations of the directional characteristics of sea waves, *Geophys. J. R. Astron. Soc.*, *17*, 93–120, 1969.
- Smith, J. A., Doppler sonar and surface waves: Range and resolution, *J. Atmos. Oceanic Technology*, *6*, 680–696, 1989.
- Terray, E. A., and L. F. Bliven, The vertical structure of turbulence beneath gently breaking wind waves, in *The Ocean Surface*, edited by Y. Toba and H. Mitsuyasu, pp. 395–400, Kluwer Academic, Hingham, MA, 1985.
- Van Heteren, J., H. Keijsers, and B. Schaap, Comparison wave directional measuring systems, *Appl. Ocean Res.*, *10*(3), 129–143, 1988.

R. T. Guza, T. H. C. Herbers, and R. L. Lowe, University of California, San Diego, Scripps Institution of Oceanography, Center for Coastal Studies, 0209, 9500 Gilman Drive, La Jolla, CA 92093-0209.

(Received March 5, 1991;  
revised May 10, 1991;  
accepted May 10, 1991.)